Caldesmon mutant defective in Ca^{2+}-calmodulin binding interferes with assembly of stress fibers and affects cell morphology, growth and motility

Yan Li, Jenny L. C. Lin, Rebecca S. Reiter, Karla Daniels, David R. Soll and Jim J. C. Lin*

Department of Biological Sciences, University of Iowa, 340 Biology Building East, Iowa City, IA 52242-1324, USA

*Author for correspondence (e-mail: jim-lin@uiowa.edu)

Accepted 10 March 2004
Journal of Cell Science 117, 3593-3604 Published by The Company of Biologists 2004
doi:10.1242/jcs.01216

Summary

Despite intensive in vitro studies, little is known about the regulation of caldesmon (CaD) by Ca^{2+}-calmodulin (Ca^{2+}-CaM) in vivo. To investigate this regulation, a mutant was generated of the C-terminal fragment of human fibroblast CaD, termed CaD39-AB, in which two crucial tryptophan residues involved in Ca^{2+}-CaM binding were each replaced with alanine. The mutation abolished most CaD39-AB binding to Ca^{2+}-CaM in vitro but had little effect on in vitro binding to actin filaments and the ability to inhibit actin/tropomyosin-activated heavy meromyosin ATPase. To study the functional consequences of these mutations in vivo, we transfected an expression plasmid carrying CaD39-AB cDNA into Chinese hamster ovary (CHO) cells and isolated several clones expressing various amounts of CaD39-AB. Immunofluorescence microscopy revealed that mutant CaD39-AB was distributed diffusely throughout the cytoplasm but also concentrated at membrane ruffle regions. Stable expression of CaD39-AB in CHO cells disrupted assembly of stress fibers and focal adhesions, altered cell morphology, and slowed cell cycle progression. Moreover, CaD39-AB-expressing cells exhibited motility defects in a wound-healing assay, in both velocity and the persistence of translocation, suggesting a role for CaD regulation by Ca^{2+}-CaM in cell migration. Together, these results demonstrate that CaD plays a crucial role in mediating the effects of Ca^{2+}-CaM on the dynamics of the actin cytoskeleton during cell migration.

Key words: Actin-bundling activity, Actin-stabilizing activity, Caldesmon, Focal adhesion, Wound-healing assay, Lamellipodium

Introduction

Calmodulin (CaM) plays a crucial role in the regulation of cell motility (Chin and Means, 2000). An increase in intracellular Ca^{2+} concentration leads to the formation of a Ca^{2+}-CaM complex that subsequently signals cell locomotion. Inhibition of the Ca^{2+}-CaM complex significantly slows migration of cultured rabbit gastric cells (Ranta-Knuuttila et al., 2002). Likewise, inhibition of CaM activity by caged peptide leads to the rapid cessation of locomotion and membrane extension in eosinophils (Walker et al., 1998). Consistent with its role in regulating cell motility, the spatial distribution of Ca^{2+}-CaM has been shown to be crucial for the extension of filopodia in growth cones (Cheng et al., 2002). Furthermore, CaM activation is greatest in lamellae at the leading edge of fibroblasts in early stages of the wound-healing process (1-4 hours after wounding), followed by a relocation to the posterior end (Hahn et al., 1992). Its involvement in the regulation of cell motility indicates that the Ca^{2+}-CaM complex is able to control the dynamics of the cytoskeleton via downstream effectors. The regulation of myosin light chain kinase (MLCK) by Ca^{2+}-CaM and its role on cell contractility have been intensively studied (Gough and Taylor, 1993; Walker et al., 1998). However, the role of the Ca^{2+}-CaM complex in actin localization and polymerization is poorly understood, although in vitro studies have demonstrated that actin filaments are regulated by Ca^{2+}-CaM (Pritchard et al., 1987) and have identified several actin-binding proteins whose activities are regulated by the Ca^{2+}-CaM complex (Shirinsky et al., 1992; Sobue et al., 1983).

One of these actin-binding proteins, caldesmon (CaD) (Smith et al., 1987) has been shown to stabilize microfilaments (Ishikawa et al., 1989a; Ishikawa et al., 1989b; Warren et al., 1994), to enhance actin binding of tropomyosin (Yamashiro-Matsumura and Matsumura, 1988) and to inhibit myosin ATPase activity in vitro (Smith et al., 1987). Most of the functional domains of CaD are located in its C-terminal half (Marston and Redwood, 1991). Previously, we subcloned the C-terminal fragment of human fibroblast caldesmon (CaD39) and demonstrated that the bacterially synthesized C-terminal fragment CaD39 retained the abilities to bind to actin, to potentiate tropomyosin binding and to inhibit myosin ATPase activity (Novy et al., 1993). When stably expressed in Chinese hamster ovary (CHO) cells, CaD39 stabilized microfilaments and protected endogenous tropomyosin from turnover (Warren et al., 1994). Furthermore, we demonstrated that the activity of force-expressed CaD39 was regulated similarly to endogenous CHO CaD (Warren et al., 1996).

The effects of CaD on the actomyosin system can be reversed in vitro by Ca^{2+}-CaM (Smith et al., 1987). Two well-conserved domains have been identified within the C-terminal half of CaD, sites A and B, that are responsible for the interaction with Ca^{2+}-CaM (Marston et al., 1994; Mezgueldi et al., 1994; Zhan et al., 1991). In human fibroblast CaD, the sequences for sites A and B are: ^{459}MWEKGNVF and

^{489}SRINEWLTK (underlined tryptophan (W) residues are the crucial residues mutated below). In human smooth muscle CaD, site A and site B localized between amino acids 715-722 and 744-752, respectively (Hayashi et al., 1992; Humphrey et al., 1992). It has been shown that the tryptophan residues within the two domains are crucial for Ca^{2+}-CaM binding (Graether et al., 1997). Despite a wealth of in vitro evidence, there is very little evidence suggesting that CaD activity is indeed regulated by Ca^{2+}-CaM in living cells or that it plays a role in controlling actin filament dynamics. To study the regulation of CaD by Ca^{2+}-CaM in vivo and to investigate further the role of CaD in Ca^{2+}/CaM-regulated cell motility, we created a CaD39 mutant, CaD39-AB, in which both of the tryptophan residues essential for Ca^{2+}-CaM binding were replaced with alanine. Here, we report that, with the exception of Ca^{2+}-CaM binding, CaD39-AB retains actin-binding properties similar to that of wild-type CaD39 and is still able to potentiate tropomyosin binding to actin and to inhibit actomyosin ATPase. Expression of CaD39-AB in CHO cells leads to disruptions of stress fibers and focal adhesions, a defect in cell morphology, and a delay in cell-cycle progression. Moreover, CaD39-AB impairs cell motility during wound healing. Cells expressing CaD39-AB migrate much more slowly than control cells and change their direction of movement more frequently than normal cells.

Materials and Methods

Construction of the CaD39-AB mutant

Point mutations were introduced into CaD39 fragment by splicing through overlapping extension (SOE) (Horton et al., 1989; Novy et al., 1993), a two-step polymerase chain reaction that replaced the tryptophan residues essential for Ca^{2+}-CaM binding with alanine residues. Briefly, CaD39 subcloned in a pCB6hx vector was amplified in two separate reactions using a pair of 5′ vector primer (5′-GGTAGGCGTGTACGGTGGGAGGTCTAT-3′) and a mutagenic primer (see below), or the complementary mutagenic primer and a 3′ vector primer (5′-TGGAGTGGCAACTTCCAGGGCCAGGA-3′). The two resulting fragments were then gel purified and used in a second round of PCR reactions with the flanking primers (5′ and 3′ vector primers) to generate either the 39CaMA or 39CaMB mutant. The double mutant CaD39-AB was generated by mixing the 39CaMA mutant with the mutagenic primers for 39CaMB in sequential PCR. After gel purification, the PCR product was digested with *Xba*I and subcloned into either the eukaryotic expression vector pCB6hx or the prokaryotic expression vector pET8c. The mutagenic primers are listed below with the mutated codon underlined.

39CaMA: 5′-CATTCCCTTTCTCCGCCATACTCTTGA-3′ and 5′-CATCAAGAGTATGGCGGAGAAAGGGAATG-3′;

39CaMB: 5′-GGTTTTAGTTAGCGCTTCATTGATGCGGC-3′ and 5′-GCATCAATGAAGCGCTAACTAAAACCCCAG-3′

Purification of recombinant proteins

Plasmids pETCaD39 and pETCaD39-AB were transformed individually into BL21(DE3)pLysS. Recombinant proteins were expressed and purified as previously described (Novy et al., 1993). Briefly, the soluble fraction of heat-treated bacteria lysate was subjected to ammonium sulfate fractionation, followed by separation of the protein mixture through two rounds of fast performance liquid column chromatography (Mono S column and Superose 12 column). Purified CaD39 and CaD39-AB proteins were identified by 12.5% sodium-dodecyl-sulfate polyacrylamide-gel electrophoresis (SDS-PAGE) and western-blot analysis with the monoclonal antibody C21 against CaD.

In vitro Ca^{2+}-CaM- and actin-binding assays

Binding of CaD39-AB or CaD39 to Ca^{2+}-CaM was performed by a modified enzyme-linked immunosorbent assay (ELISA) as previously described (Lin et al., 1991). 100 μl of a 5 μg ml^{-1} solution of bovine brain calmodulin (Sigma-Aldrich, St Louis, MO) was added to wells of Immulon II microtiter plate and incubated overnight at 4°C. After removing excess Ca^{2+}-CaM, an increasing amount of either CaD39 or CaD39-AB was added into the wells and incubated at 37°C for 30 minutes. The wells were washed three times with PBS-Tween-Ca^{2+} (10 mM sodium phosphate buffer, pH 8.2, 0.15 M NaCl, 0.05% Tween-20, 0.2 mM $CaCl_2$). Bound CaD39 or CaD39-AB was then incubated with the monoclonal antibody C21 against CaD (used at 1000-fold dilution) at 37°C for 30 minutes. After washing three times with PBS-Tween-Ca^{2+}, the wells were incubated for an additional 30 minutes at 37°C with horseradish-peroxidase-conjugated anti-mouse IgG at 1000-fold dilution. The enzyme activity in each well was detected by adding substrate ABTS [0.03% H_2O_2 and 1 mM 2,2′-azino-*bis*(3-ethylbenzothiazoline-6-sulfonate acid) in 0.1 M citrate buffer, pH 4.2] and assaying the color intensities at 405 nm using an ELISA reader (SpectraMax Plus, Molecular Devices, Sunnyvale, CA).

Actin binding abilities of the recombinant proteins were measured in a cosedimentation assay (Novy et al., 1993). 9.3 μM actin filaments were incubated with various amounts of CaD39 or CaD39-AB in binding buffer containing 10 mM imidazole buffer (pH 7.0), 30 mM KCl, 0.1 mM EGTA and 1 mM DTT. After incubation at room temperature for 40 minutes, the reaction mixtures were centrifuged at 130,000 ***g*** for 30 minutes in an airfuge. The pellet from each reaction was resuspended in binding buffer. Both the supernatants and the corresponding pellets were analysed by 12.5% SDS-PAGE after they were dissolved in SDS sample buffer. The proteins were stained with Coomassie Blue, scanned and analysed using Scion Image software (Scion, Frederick, MD). Additional actin-binding assays were performed by incubating 3.6 μM recombinant human fibroblast tropomyosin isoform 3 (hTM3) (Novy et al., 1993), 9.3 μM F-actin and 0.5 μM CaD39 or CaD39-AB under similar conditions.

Heavy meromyosin ATPase assay

ATPase activities were measured at 29°C as described previously (Novy et al., 1993) in 20 mM imidazole buffer, pH 7.0, 50 mM KCl, 2 mM $MgCl_2$, 1 mM dithiothreitol, 0.1 mM EGTA, 0.04 μM rabbit skeletal heavy meromyosin (HMM; Cytoskeleton, Denver, CO), 12 μM skeletal muscle actin, 2.5 μM recombinant human tropomyosin isoform 5 (hTM5) and 2.8 μM CaD39 or CaD39-AB. The reactions were started by the addition of 1 mM ATP containing 5 μCi [γ-^{32}P]-ATP. In the reversal of CaD inhibition, 2.5 μM CaM and 2 mM Ca^{2+} were included in the reaction.

Cell transfection and immunofluorescence microscopy

CHO cells were cultured in Dulbecco's modified Eagle's medium (DMEM) plus 10% fetal bovine serum (FBS) at 37°C in 5% CO_2. Plasmid DNA was introduced into CHO cells using Lipofectamine reagent (Invitrogen, Carlsbad, CA). 24 hours after transfection, cells were selected in DMEM plus FBS medium containing 500 μg ml^{-1} G418 (Gibco, Gaithersburg, MD). For establishing stable clones expressing CaD39-AB, single cells were cloned after 2 weeks of drug selection. Each cell clone was expanded and tested for expression of CaD39-AB. Stable lines m4-65 and m5-8 were selected for this study. The nonexpressing G418-resistant cell line C3 was used as an experimental control. A previously isolated stable line 39C15 that expresses wild-type CaD39 was also included for comparison in this study (Fig. 1). To detect the expression of force-expressed protein in CHO cells, the monoclonal antibody C21 (Lin et al., 1991) was used in immunofluorescent microscopy. As described before (Li et al., 2003), C21 antibody only recognized overexpressed exogenous

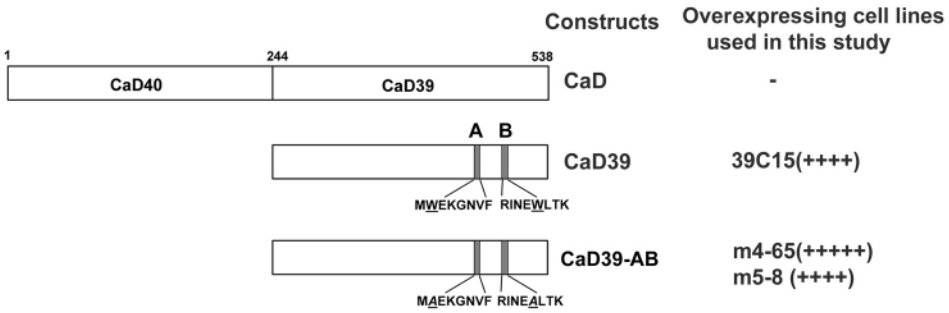

Fig. 1. Constructs of human fibroblast caldesmon (CaD) and their corresponding expressing cell lines used in this study. The C-terminal fragment (CaD39) consists of amino acids 244 to 538. Ca^{2+}/CaM-binding domains are labeled as gray boxes and their amino acid sequences are listed. The italic underlined letters represent the replacement of tryptophan residues with alanine in the Ca^{2+}/CaM-binding-site-defective mutant (CaD39-AB). The expression levels of various constructs relative to endogenous CHO CaD in each stable cell lines are indicated by the number of + signs in parentheses.

proteins when used at 1000-fold dilution. To detect focal adhesions, cells were stained with anti-vinculin monoclonal antibody (Sigma-Aldrich, St Louis, MO) at a 300-fold dilution. To examine the organization of stress fibers, fixed and permeabilized cells were incubated with rhodamine-conjugated phalloidin (Molecular Probes, Eugene, OR). The fluorescent staining was visualized using confocal microscopy. *z*-Axis series of *xy* optical planes were obtained at 0.2 μm intervals using a BioRad Radiance 2100MP (BioRad, UK). Projections and merged images were constructed using the co-localization module Laser Sharp 2000 software (BioRad, UK).

Analysis of cell migration during wound healing

Confluent cells were wounded by scraping the coverslip with a sterile pipette. After 1 hour of recovery in a 37°C incubator, the coverslip was transferred to a Dvorak-Stotler perfusion chamber (Lucas-Highland, Chantilly, VA) that positioned on the stage of a Zeiss inverted microscope prewarmed to 35°C. Cell behavior was monitored for 5 hours through a 40× objective and a high performance CCD camera (Optronics, Galito, CA). Images were digitized directly onto the hard drive of a Macintosh computer equipped with a Data Translation frame grabber board (Data Translation, Marlboro, MA) and 2D-DIAS software. Cells at the leading edge were manually traced and the perimeters converted to β-spline replacement images that were used to compute the positions of the cell centroids (Soll, 1995). Methods for computing parameters derived from 2D-DIAS have been presented elsewhere (Soll, 1995; Soll and Voss, 1998). Parameters for cell motility, including velocity, net path length, directional change and persistence, were computed from the position of the cell centroid. Area, a parameter of cell shape, is defined as the area of the final shape at frame *n* minus the area of any holes. Roundness is a percentage measure of how efficiently a given amount of perimeter encloses the area. A circle has the largest area and has a roundness of 100%. 'Positive flow', a measure of the area change per unit, was calculated by overlapping cell outlines between frames *n* and *n*–1. The regions in frame *n* not contained in frame *n*–1 were considered to be 'expansion zones'. The summed area of expansion zones divided by the total cell area in frame *n* multiplied by 100 represents the positive flow. Likewise, the summed area of 'contraction zones' divided by the total cell area in frame *n* multiplied by 100 represents 'negative flow'.

Other procedures

Tropomyosin-enriched actin filaments were isolated from 15 100-mm dishes of 39C15 and 16 150-mm dishes each of m5-8 and m4-65 as previously described (Lin et al., 1984). Briefly, the cytoskeleton of interphase cells was extracted in KTG solution (0.1 M PIPES, pH 6.9, 5 mM $MgCl_2$, 0.2 mM EGTA, 0.05% Triton X-100, 4 M glycerol) and homogenized in the presence of 5 mM ATP and 5 mM Mg^{2+}. After centrifugation at 10,000 ***g***, the supernatant was incubated with anti-tropomyosin monoclonal antibody. Tropomyosin-enriched filaments were pelleted by low-speed centrifugation (10,000 ***g***) and analysed by western blots using C21 antibody. The loading volumes were adjusted among different expressing cell lines so that equivalent amounts of the tropomyosin-enriched microfilaments were later analyzed by western blot. As demonstrated previously, the yield of tropomyosin-enriched microfilaments isolated by this method is roughly proportional to the amount of stress fibers in the cells (Lin et al., 1984; Matsumura et al., 1983), indicating that this method preferentially isolates actin bundles. Growth rates for various cell lines were determined by inoculating cells that are exponentially growing into 60-mm dishes. The initial cell number was 4×10^4 cells per dish. One dish was harvested every 24 hours for determination of cell numbers.

Results

Binding ability of CaD39-AB to Ca^{2+}-CaM is greatly reduced by the mutation

It was shown previously that two Trp residues at the C-terminal fragment of human fibroblast CaD (CaD39), W460 and W494, were crucial for Ca^{2+}-CaM binding (Graether et al., 1997). Using site-directed mutagenesis, a mutant of the CaD39 fragment was generated in which both W460 and W494 were substituted with alanine, and named CaD39-AB (Fig. 1). To characterize its in vitro binding properties, CaD39-AB and the wild-type CaD39 fragment were bacterially expressed and purified as described previously (Li et al., 2003). The purified proteins were subjected to a Ca^{2+}-CaM binding assay using a modified ELISA method (Lin et al., 1991). In the presence of Ca^{2+}, wild-type CaD39 was able to bind to CaM (Fig. 2). The binding was EGTA sensitive (data not shown) (Lin et al., 1991). Replacing the tryptophan residues with alanine almost entirely abolishes the binding of CaD39-AB to Ca^{2+}-CaM (Fig. 2).

CaD39-AB retains the ability to bind to actin filaments and to inhibit myosin ATPase activity

Actin-binding ability of CaD39-AB was examined in a cosedimentation assay in which the purified protein CaD39-AB or CaD39 was incubated with skeletal muscle F-actin. After high-speed centrifugation, comparable amounts of CaD39-AB and CaD39 were detected in the pellet fractions (Fig. 3A,B), whereas neither CaD39 nor CaD39-AB was detected in pellet fractions in the absence of actin filaments (data not shown). Further quantitative analyses in three additional experiments revealed no significant differences between CaD39-AB and the wild-type CaD39 in either the affinity or the kinetics of actin binding (Fig. 3C), suggesting that the actin binding ability was

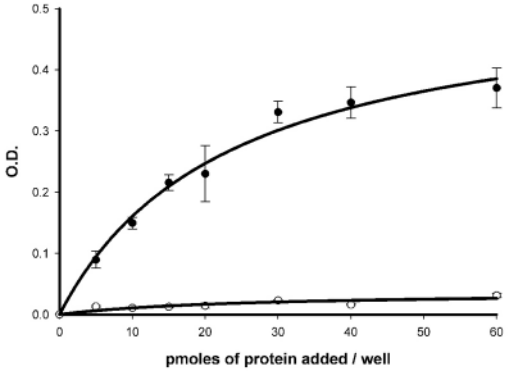

Fig. 2. Binding of CaD39 and CaD39-AB to CaM. The binding of either CaD39 (filled circles) or CaD39-AB (open circles) to CaM was measured by a modified ELISA method (Lin et al., 1991). Wells in microtiter plate were coated with 100 μl of 5 μg ml^{-1} bovine brain CaM at 4°C overnight. Bound Ca^{2+}-CaM was incubated with increasing amounts (0-60 pmole) of CaD39 or CaD39-AB, subsequently with monoclonal antibody C21 against CaD, and then with horseradish-peroxidase-conjugated anti-mouse IgG. After a 30-minute incubation with substrate (ABTS), the color intensity (O.D.) was determined by an ELISA reader at 405 nm. Averages from three independent experiments were plotted in the figure, with error bars representing the standard deviation. Mutant CaD39-AB almost abolished its binding to Ca^{2+}-CaM, whereas wild-type CaD39 binds to Ca^{2+}-CaM in a saturable fashion.

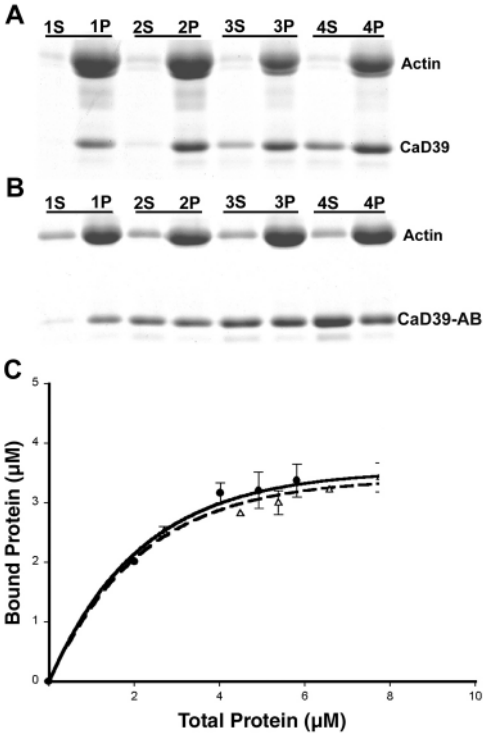

Fig. 3. Actin binding of CaD39 or CaD39-AB. Recombinant protein CaD39 at 2.01 μM, 4.02 μM, 4.47 μM, 4.92 μM (A) or CaD39-AB at 2.68 μM, 5.37 μM, 5.82 μM, 7.76 μM (B) was incubated with 9.3 μM F-actin in 10 mM imidazole buffer (pH 7.0) containing 30 mM KCl, 0.1 mM EGTA and 1 mM DTT. After incubation and subsequent centrifugation, both supernatants and pellets were adjusted to equivalent volumes and analysed by SDS-PAGE. 'S' and 'P' represent the supernatant (free) and pellet (bound) fraction, respectively, of CaD in each reaction. The binding data from three independent experiments were quantified using Scion Image software (C), which showed no significant difference of actin-binding ability between CaD39 and CaD39-AB.

not affected by the mutation at the Ca^{2+}-CaM binding sites. We previously found that CaD39 potentiated actin binding of tropomyosin (Novy et al., 1993). Therefore, we further examined the actin-binding affinities of recombinant hTM3 in the presence of CaD39 or CaD39-AB. As shown in Fig. 4, in a low salt concentration (30 mM KCl and no Mg^{2+}), where hTM3 alone barely binds to actin (Fig. 4, 1S and 1P), the addition of either CaD39 or CaD39-AB greatly increased the amount of hTM3 bound to actin filaments (Fig. 4, 2P and 3P), suggesting that the ability of the mutant to enhance actin binding of tropomyosin is similar to that of the wild-type CaD39 fragment and intact CaD protein (Novy et al., 1993).

The ability of CaD39-AB to inhibit actin/tropomyosin-activated HMM ATPase activity was compared with that of wild-type CaD39 using a myosin HMM ATPase assay as described previously (Novy et al., 1993). As shown in Fig. 5, the actin/tropomyosin-activated HMM ATPase activity decreased by 49.2% in the presence of 2.8 μM wild-type CaD39. The inhibition of ATPase by CaD39 could be reversed by 2.5 μM Ca^{2+}-CaM. Similarly, CaD39-AB inhibited the actin/tropomyosin-activated HMM ATPase to about 42.6% of the control activity in the absence of CaD (Fig. 5). This inhibition could not be significantly reversed by the addition of Ca^{2+}-CaM. These results suggest that the ability of CaD39-AB to inhibit myosin ATPase is neither impaired by the mutations at the Ca^{2+}-CaM binding sites nor effectively reversed by the addition of Ca^{2+}-CaM.

Stable expression of CaD39-AB in CHO cells interferes with the organization of stress fibers and focal adhesions

To investigate the consequences of expressing CaD39-AB in CHO cells, we generated stable clones expressing the mutant fragment. After transfection and cell cloning, cell lines C35, C41, m4-2, m5-8 and m4-65 were obtained, expressing low to high amounts of exogenous protein (Fig. 6A). Two overexpressing clones, m5-8 and m4-65, were used for further characterization of the cells expressing CaD39-AB, and the nonexpressing drug-resistant line C3 served as a negative control. To verify that mutant phenotypes observed in the overexpressing cells resulted from expression of CaD39-AB rather than that of wild-type CaD39, we also included a CaD39-overexpressing cell line, 39C15 (Warren et al., 1994) for comparison. The stable clones used in this study are summarized in Fig. 1.

To detect the localization of CaD39-AB in the stably expressed cell lines, we used immunofluorescent microscopy with monoclonal antibody C21 against the C-terminal fragment of CaD (Lin et al., 1991). When used at a 1000-fold dilution, C21 antibody could only detect the presence of overexpressed exogenous proteins in the stable clones (Fig. 7E,H), but barely any cross-reactivity could be detected with endogenous CHO CaD in nonexpressing C3 cells (Fig. 7B). Consistent with previous findings (Warren et al., 1994), the

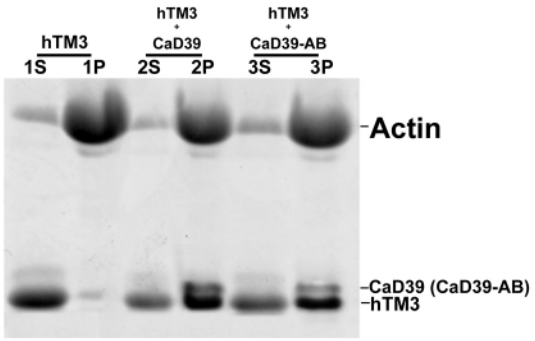

Fig. 4. Both CaD39 and CaD39-AB potentiate the actin binding of tropomyosin. Using the same buffer conditions as in Fig. 3, 9.3 μM F-actin and 3.6 μM hTM3 were incubated alone (1S and 1P), with 0.5 μM CaD39 (2S and 2P) or with 0.5 μM CaD39-AB (3S and 3P). After incubation and subsequent centrifugation, both supernatants (S) and pellets (P) were dissolved and analysed by SDS-PAGE. Like wild-type CaD39, mutant CaD39-AB protein potentiated tropomyosin binding to actin filaments.

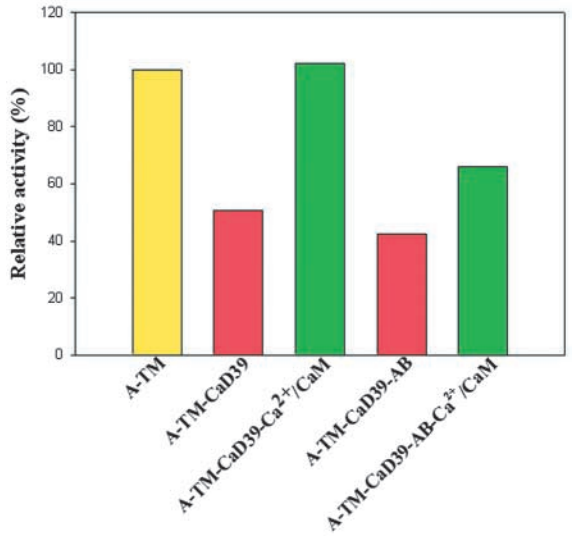

Fig. 5. Inhibition of actin/tropomyosin-activated HMM ATPase by CaD39 and CaD39-AB. Rates of HMM ATPase were measured at 29°C in 20 mM imidazole buffer (pH 7.0), 2 mM $MgCl_2$, 50 mM KCl, 0.1 mM EGTA and 1 mM DTT. 12 μM F-actin, 2.5 μM hTM5 and 0.04 μM HMM were incubated in the absence or presence of 2.8 μM CaD39 or CaD39-AB. The reversal of CaD inhibition was measured in the presence of 2.5 μM CaM and 2 mM $CaCl_2$. The actin/tropomyosin-activated HMM ATPase activity (4.58 nmole phosphate released per minute per mg of HMM) obtained under this assay condition was used as 100%. Abbreviations: A, actin; TM, tropomyosin.

overexpressed CaD39 protein was found on stress fibers and ruffle regions of 39C15 cells (Fig. 7E,F). By contrast, CaD39-AB in m4-65 cells displayed diffuse staining throughout the cytoplasm but seemed to concentrate at ruffle regions (Fig. 7H). Surprisingly, the expressed CaD39-AB was not found on stress fibers counter-stained with rhodamine-labeled phalloidin (Fig. 7I). This staining pattern of CaD39-AB was observed in all the isolated stable clones irrespective of the expression level (data not shown). Furthermore, the transiently expressed

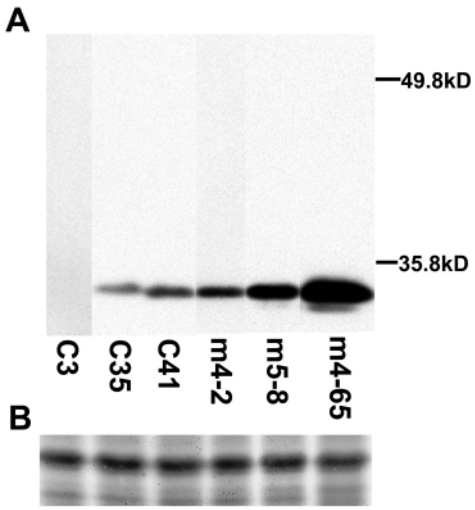

Fig. 6. Stable clones expressing CaD39-AB. Total proteins were prepared from five independent stable cell lines (C35, C42, m4-2, m5-8 and m4-65) and a non-expressing cell line C3. Equivalent amounts of protein extract were resolved using SDS-PAGE and the portion of the Coomassie-Blue-stained gel was shown (B) to indicate the equal loading in the gel. The expression levels of CaD39-AB in the stable clones were analysed by western blot (A).

CaD39-AB mutant (36 hours after transfection) also showed a diffuse staining pattern and did not incorporate into the stress fibers (data not shown). Compared with the control cells, phalloidin staining is more prominent in 39C15 cells (Fig. 7F), suggesting that CaD39 stabilizes the structure of stress fibers (Warren et al., 1996). However, the stress fiber structure in CaD39-AB-expressing cells appears to be disintegrated (Fig. 7I).

The observation that CaD39-AB was not associated with stress fibers was further supported by the isolation of tropomyosin-enriched microfilaments. When tropomyosin-enriched actin bundles were isolated and analysed on Coomassie-Blue-stained gels (Fig. 8B) and western blots (Fig. 8C-E), the amounts of associated tropomyosin 5 (TM5) in both 39C15 and m4-65 cells was very similar (Fig. 8D). However, after calculating the differences in the initial cell numbers used for the actin bundle isolation and in the volumes loaded in the gel, we found that the yield of actin bundles isolated from m4-65 cells was 2.2-times less than that isolated from 39C15 cells. Furthermore, the amount of associated CaD39-AB in either the m5-8 or m4-65 cells (Fig. 8C, lane 2, and Fig. 8C,E, lane 3) was significantly lower than that of CaD39 in the 39C15 clone (Fig. 8C,E, lane 1). The total amount of CaD39-AB expressed in the clone m5-8 was comparable to that of CaD39 expressed in the isolated CaD39-expressing clone 39C15, whereas the amount of CaD39-AB in m4-65 was significantly higher (Fig. 8A). We have previously demonstrated that the molar ratio of the exogenous CaD39 to the endogenous CaD protein is about 80 in the 39C15 cells (Warren et al., 1994). Therefore, the expression level of CaD39-AB in m5-8 and m4-65 were no less than 80 times higher than that of the endogenous CHO CaD. Overall, these data demonstrate that force-expressed CaD39-AB is unable to bind stress fibers, whereas CaD39 is readily incorporated into stress fibers. Because the in vitro binding

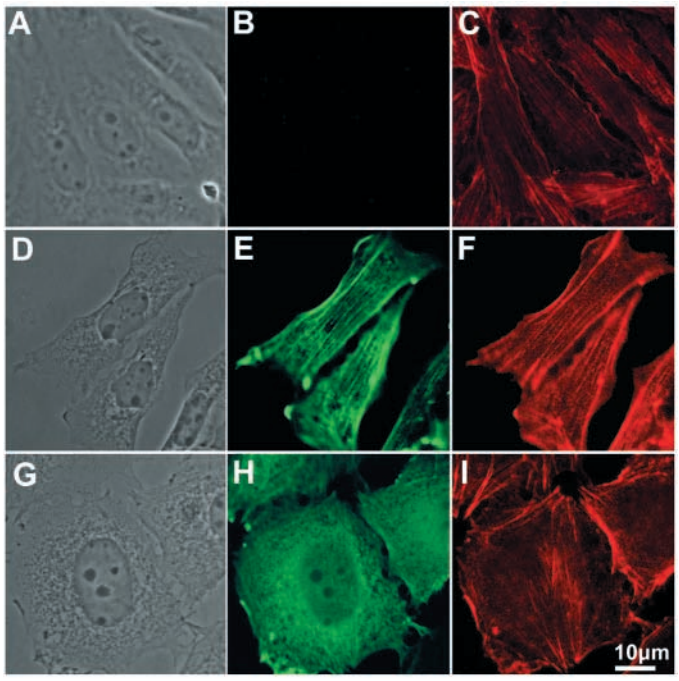

Fig. 7. Distribution of CaD39-AB in overexpressing clones. Cultured cells from different clones were stained with C21 antibody (B,E,H) and phalloidin (C,F,I). (A-C) Control cells from non-expressing clone C3. (D-F) 39C15 cells overexpressing wild-type CaD39. (G-I) m4-65 cells overexpressing CaD39-AB. When used at 1000-fold dilution, C21 antibody could not detect the endogenous CHO CaD (B) and only the localization of overexpressed exogenous proteins could be visualized (E,H). Although wild-type CaD39 incorporated into stress fibers (E), mutant CaD39-AB diffused throughout the cells and was relatively concentrated at many small ruffle regions (H). In addition to cell shape changes, the stress fiber arrays were disrupted in CaD39-AB-overexpressing cells (I). Scale bar, 10 μm.

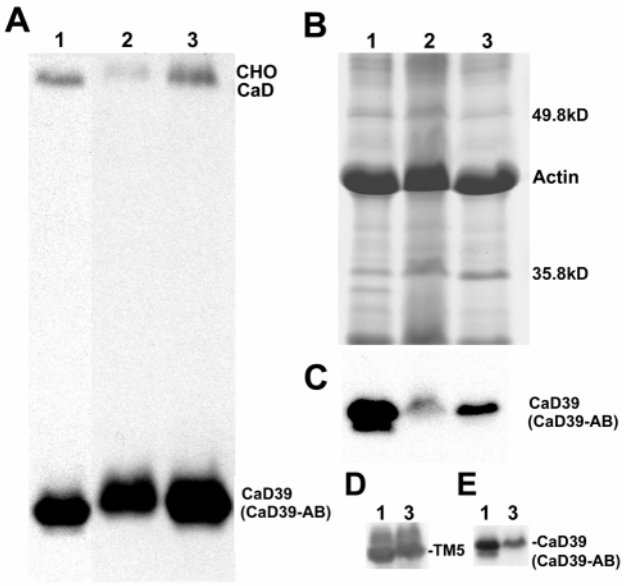

Fig. 8. Actin bundles isolated from CaD39-AB-expressing cells contain much less force-expressed protein than that from CaD39-expressing cells. Lane 1, 39C15; lane 2, m5-8; lane 3, m4-65. (A) Western blot analysis of total protein extract from 39C15, m5-8 and m4-65 using C21 anti-CaD antibody. (B) SDS-PAGE analysis of tropomyosin-enriched actin bundles isolated from interphase cells of 39C15, m5-8 and m4-65. (C-E) Western blot analyses of isolated tropomyosin-enriched actin bundles with C21 antibody (C,E) and with CG3 anti-TM5 antibody (D). Despite the comparable CaD expression levels, the portion of the force-expressed protein associated with actin bundles was much less in both m5-8 and m4-65 cells than that in 39C15 cells. After calculating the differences in the initial cell numbers used for the actin bundle isolation and in the volumes loaded in the gel, the yield of actin bundles isolated from m4-65 cells was 2.2 times lower than that for 39C15 cells.

assay revealed that actin-binding affinity of CaD39-AB was not impaired, it is possible that CaD39-AB is still able to bind actin filaments in vivo but that those CaD39-AB-containing microfilaments are somehow prohibited from forming stress fibers. In support of this suggestion, when total cytoskeletal extracts were analysed by western blot, the amount of CaD39-AB associated with total actin filaments was comparable to that of CaD39 in overexpressing cells (data not shown).

To investigate whether CaD39-AB is able to disrupt the assembly of stress fibers and focal adhesions, we double-labeled the cells of the overexpressing clone m4-65 with phalloidin and an anti-vinculin monoclonal antibody. As shown in Fig. 9, control C3 cells displayed straight, well-developed stress fibers across the cell bodies (Fig. 9A). Similar phalloidin staining patterns were also observed in CaD39-overexpressing 39C15 cells (Fig. 9E). By contrast, stress fibers in CaD39-AB-overexpressing cells were short, fragmented and abnormally localized to cell peripheries (Fig. 9I). The tropomyosin localization revealed by anti-tropomyosin antibodies (CG3 and LC24) in these CaD39-AB-expressing cells was very similar to stress-fiber staining pattern (data not shown). In agreement with the actin organization, staining of vinculin revealed that focal adhesions in both the control cells and the cells expressing wild-type CaD39 exhibited linear organization along stress fibers (Fig. 9B,F). Prominent vinculin staining could be observed at both ends of the stress-fiber arrays (Fig. 9C,D,G-H). In m4-65 cells, vinculin-containing focal adhesions appeared more prominently at cell peripheries, whereas those inside the cell bodies were mostly small and punctate (Fig. 9J,K). Moreover, most of the focal adhesions at cell peripheries did not overlap with stress fibers (Fig. 9K), although these two structures were usually in close proximity (Fig. 9L). Excluding the cortical region, CaD39-AB-overexpressing cells often exhibited no or weak focal-adhesion structures at the tips of stress fibers (Fig. 9L), suggesting that formation/maturation of focal adhesions was impaired by the disruption of stress fibers in overexpressing cells.

Overexpression of CaD39-AB affects cell morphology and causes cell cycle delays

Under phase-contrast microscopy, we observed significant changes in cell shape in CaD39-AB-overexpressing cells compared with either wild-type CHO or CaD39-overexpressing cells (Fig. 7). To characterize better the morphological defects, cells from clones m5-8 and m4-65, as well as cells from clone 39C15, were seeded in culture dishes so that similar cell densities were obtained after 2 days of

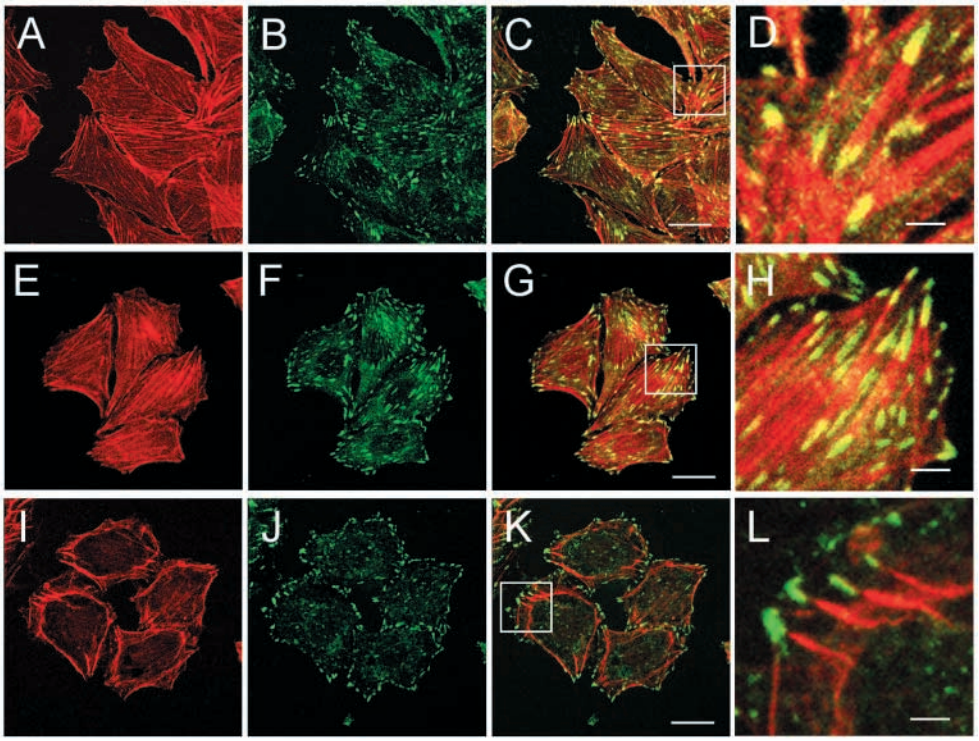

Fig. 9. Effects of CaD39-AB expression on stress fibers and focal adhesions. (A-D) Control C3 cells. (E-H) 39C15 cells expressing CaD39. (I-L) m4-65 cells expressing CaD39-AB. Double staining was performed with phalloidin (A,E,I) and anti-vinculin monoclonal antibody (B,F,J). (C,G,K) Merged images of A and B, E and F, and I and J, respectively. Representative areas in C, G and K are highlighted in boxes and enlarged in D, H and L, respectively. Scale bars, 15 μm (C,G,K), 3 μm (D,H,L).

Table 1. Cell size analysis

Cell lines	Cell number	Area (μm²)	Roundness (%)
39C15[1]	184	619.89±254	0.36±0.10
m5-8[2]	161	977.01±348	0.42±0.11
m4-65[3]	120	1106.64±537	0.47±0.10
P value* (1 vs 2)		<0.0001	<0.0001
P value (1 vs 3)		<0.0001	<0.0001

*Student's *t*-test was performed to calculate the *P* value if the samples passed the test of normality and equal variance. Otherwise, the rank sum test was used.

culture. After fixation, the area and roundness of each individual cell were quantified using the 2D-DIAS software program (Soll and Voss, 1998). As shown in Table 1, cells from both m5-8 and m4-65 clones were significantly larger and rounder than those of clone 39C15. However, 39C15 cells showed no difference from parent CHO cells in cell morphology (Warren et al., 1994). The severity of the morphological defects roughly paralleled the expression levels of CaD39-AB (Table 1), demonstrating that changes in cell shape are caused by the expression of CaD39-AB.

While culturing, we noticed that the CaD39-AB-expressing clones grew slowly. To determine whether there was a cell-cycle defect in CaD39-AB-expressing clones, we measured growth rate. We found that the number of 39C15 cells increased at a rate similar to that of CHO cells (Warren et al., 1994) (R. D. Eppinga and J.J.-C.L., unpublished). By contrast, the number of cells in both the m4-65 and m5-8 lines increased more slowly (Fig. 10). The cell doubling times of the 39C15, m5-8 and m4-65 clones were 16 hours, 21 hours and 24 hours, respectively, indicating that the expression of CaD39-AB mutant suppresses cell growth.

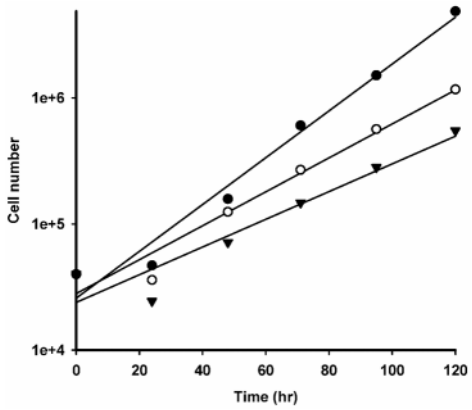

Fig. 10. Effects of CaD39-AB on cell growth. 4×10^4 39C15 (filled circles), m5-8 (open circle) and m4-65 (filled triangles) cells were plated on 60-mm dishes. Cells from each plate were trypsinized and counted every 24 hours. Cell numbers were plotted against culturing time. Calculated doubling times for 39C15, m5-8 and m4-65 were 16 hours, 21 hours and 24 hours, respectively. The expression level of mutant CaD39-AB protein was inversely proportional to growth rate.

Overexpression of CaD39-AB affects cell motility in a wound-healing assay

To investigate whether overexpression of CaD39-AB affects cell movement, cells from the non-expressing cell line (C3) and the overexpressing cell lines (m4-65 and m5-8) were analysed for cell motility in a wound-healing assay. Using the 2D-DIAS software program, motility parameters were quantified. The average of each parameter is presented in Table 2. CaD39-AB-overexpressing cells were significantly slower than control cells. Furthermore, in overexpressing cells the persistence

Fig. 11. Centroid tracks of control C3 (A) and mutant m4-65 cells (B) during wound healing. The interval between adjacent centroid is 5 minutes. Persistent, rapid movement in C3 cells was reflected by a linear track and well-separated centroids with time (A). By contrast, little translocation with frequent direction change in mutant m4-65 cells was represented by a zigzag track and clusters of centroids with time (B). Scale bar, 10 μm.

(velocity/directional change) was significantly reduced and directional change was significantly higher when translocating, suggesting that they turn more frequently than control cells. These motility defects were apparent in a comparison of centroid tracks (Fig. 11). Over a 4-hour period after wounding, the centroid tracks of translocating m4-65 cells were short and jagged. Compared with m4-65 cells, the centroid paths of control cells were longer and had more persistent directions. Similar defects were observed in another CaD39-AB-expressing cell line, m5-8 (Table 2). In contrast to CaD39-AB-expressing cells, no motility defects were detected in 39C15 cells overexpressing the wild-type CaD39 fragment (Warren et al., 1996). Taken together, these results demonstrated that expression of a CaD39 defective in Ca^{2+}-CaM binding impairs speed and directionality during wound healing.

We further examined the dynamics of lamellipodia extension during wound healing. Figs 12 and 13 show time-lapse images of migrating cells from C3 and m5-8 clones, respectively. Consistent with the characterization of lamellipodia dynamics previously demonstrated in normal fibroblasts (Fisher et al., 1988), control C3 cells extended a thin lamellipodium along the substrate, typically along the entire free edge of the wound (Fig. 12A). Difference pictures of representative control cell (Fig. 12A, arrow) with color-coded lamellipodia are shown in Fig. 12B. In contrast to control cells, cells overexpressing CaD39-AB failed to form continuous lamellipodia in the direction of the wound (Fig. 13A). Instead, multiple small, discrete protrusions were observed at the edges of these cells, each extending and retracting independently (Fig. 13B). Consistent with the observed defects in expansion zones in difference pictures, the parameters of positive flow and negative flow, measures of expansion areas and contraction areas, were significantly lower in mutant cells expressing CaD39-AB compared with that in control C3 cells (Table 2).

Discussion

Ca^{2+}-CaM binding sites and actin-binding sites can be functionally separated

In early studies, two opposing theories were proposed regarding the mechanism for the regulation of CaD by Ca^{2+}-CaM (Sobue et al., 1983; Smith et al., 1987). In the ‘flip-flop’ model (Sobue et al., 1983), Ca^{2+}-CaM competes with actin for the binding sites on CaD and therefore reverses the inhibitory effects of CaD on actomyosin ATPase by dissociating it from actin filaments. In favor of this model, the Ca^{2+}-CaM binding domain has been shown to be juxtaposed to the actin-binding domain (Fraser et al., 1997; Huber et al., 1998a; Wang et al., 1997). By contrast, the ‘four state’ model (Smith et al., 1987) proposes that Ca^{2+}-CaM can reverse the inhibitory effects of CaD by two means: either by dissociating CaD from the actin filaments or by forming an uninhibited ternary complex of Ca^{2+}-CaM-CaD-actin-tropomyosin. The fact that mutant CaD39-AB protein defective in Ca^{2+}-CaM binding retains the actin-binding ability militates against the ‘flip-flop’ model. Instead, it suggests that the binding sites for actin and Ca^{2+}-CaM are independent of each other and, therefore, that Ca^{2+}-CaM might be able to reverse the inhibitory effect of CaD on microfilaments without completely abolishing its binding to actin-tropomyosin. Consistent with our result, Helfman et al. (Helfman et al., 1999) reported that transiently transfected non-muscle CaD remained associated with stress fibers even when CaD activity was suppressed by Ca^{2+}-CaM. Recent studies of the thin filaments have indicated a more complex mechanism for CaM regulation of CaD activity in the smooth muscle cells. Notarianni et al. (Notarianni et al., 2000) have isolated, from smooth-muscle thin filaments, a structurally novel CaM that can bind to CaD in the absence of Ca^{2+}. This might indicate the presence of another inhibitory state of CaM-CaD-actin-tropomyosin complex that appears to be more sensitive to Ca^{2+} concentration change than

Table 2. Cell motility during the wound-healing assay

Cell lines	Cell number	Velocity (μm min^{-1})	Net path length (μm)	Direction change (°)	Persistence (μm/min^{-1} deg^{-1})	Positive flow (%)	Negative flow (%)
C3[1]	20	0.18±0.04	25.82	59.82±10	0.04±0.01	8.75±1.91	7.89±1.75
m5-8[2]	9	0.13±0.02	11.40	70.1±5.9	0.02±0.01	6.10±0.97	5.94±0.76
m4-65[3]	12	0.15±0.02	10.72	73.78±7.1	0.03±0.01	7.23±1.6	6.80±1.55
P value* (1 vs 2)		0.0007	<0.0001	0.0002	0.0013	0.0002	<0.0001
P value (1 vs 3)		0.0112	<0.0001	<0.0001	0.0001	0.0162	0.0222

*Student’s *t*-test was performed to calculate the *P* value if the samples passed the tests of the samples for normality and equal variance.

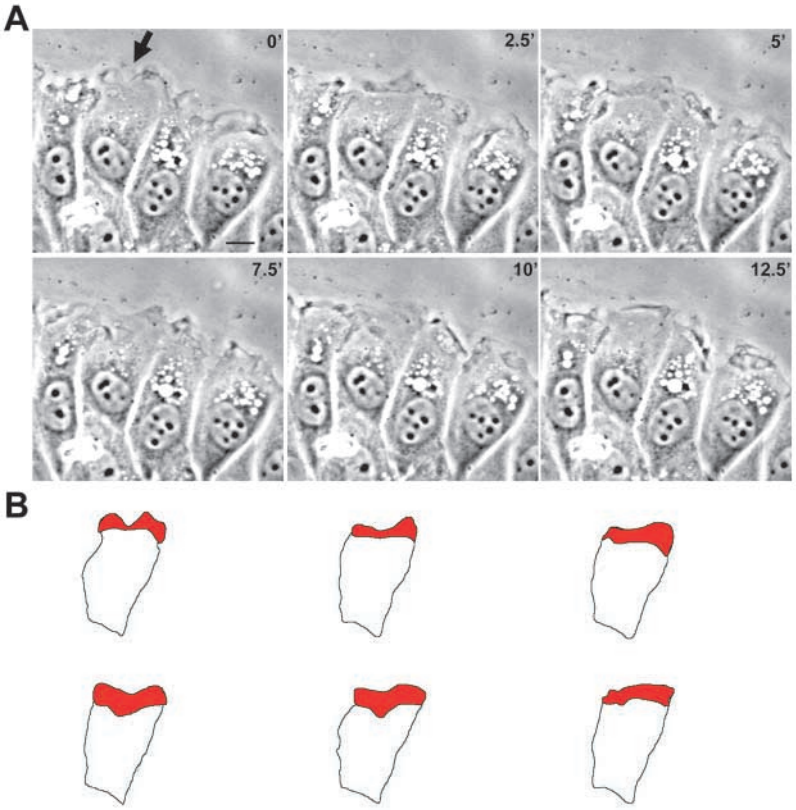

Fig. 12. Phase-contrast images and outlines of migrating control C3 cells during wound healing. Derived from original video taping, the phase-contrast images (A) of migrating cells starts 2.5 hours after wounding and continues for 12.5 minutes at intervals of 2.5 minutes. (B) The outlines of a representative cell (A, arrow) in which membrane extension zones are filled with red. A single membrane sheet covering nearly the entire leading edge was actively extending and retracting during the 12.5-minute period. Scale bar, 10 μm.

the CaD-actin-tropomyosin complex. It was proposed that, when associated with small amount of Ca^{2+}, the complex of the novel CaM and CaD could rearrange itself, which would in turn allow the actin-tropomyosin quickly to alter its conformation and to activate myosin ATPase activity (Marston et al., 1998). Whether this novel isoform of CaM also exists in non-muscle cells remains to be determined.

The CaD domains for myosin ATPase inhibition have been mapped to the C-terminal half of full-length CaD (Wang and Chacko, 1996), three of which overlap with the actin-binding sites. The mutations at Ca^{2+}-CaM-binding sites used in this study neither disrupt actin binding nor interfere with the ability to inhibit actomyosin ATPase. Interestingly, Huber et al. (Huber et al., 1998a) have generated a mutant of the 10 kDa C-terminal fragment of chicken gizzard CaD Cg1 whose activity could not be regulated by Ca^{2+}-CaM. Although the actin binding was not impaired by the mutation, the ability of Cg1 to inhibit myosin ATPase activity was significantly reduced. The difference in the ability to inhibit myosin ATPase by Cg1 and CaD39-AB is probably due to the different natures of mutants. In addition to the replacement of the tryptophans at site B, Cg1 also bore mutations of another five amino acids that flanked the tryptophan residue (Huber et al., 1998b). It is likely that mutation of these adjacent residues, rather than the mutations of the tryptophan itself, caused the decrease in the inhibition of myosin ATPase activity.

CaD has dual functions in regulating the dynamics of stress fibers

CaD39-AB displays a similar binding ability to actin filaments in vitro, just as the wild-type CaD39 does, yet it is not incorporated into stress fibers when force-expressed in CHO cells. Moreover, it appears to disrupt the organization of stress fibers and focal adhesions in overexpressing cells. It is likely that the CaD39-AB still binds to microfilaments in vivo but prevents them from forming actin bundles by bundling proteins. In support of this notion, Ishikawa et al. (Ishikawa et al., 1998) have shown in vitro that, together with tropomyosin, CaD completely prevents the bundling protein fascin from binding to actin filaments and thus inhibits its actin-bundling activity. Inhibition of actin bundling by CaD and tropomyosin can be reversed by the addition of Ca^{2+}-CaM, suggesting that regulation of CaD by Ca^{2+}-CaM plays an important role in controlling the actin-bundling activity of fascin.

We have previously reported that stress fibers in CaD39-overexpressing cells become more resistant to disruption by cytochalasin (Warren et al., 1994), suggesting a role for CaD in stabilizing stress fibers. A similar result was obtained in the transient transfection of full-length CaD, in which expression of exogenous CaD led to the formation of thicker stress fibers (Yamashiro et al., 2001). We propose that CaD serves dual functions in the regulation of stress fiber assembly. First, CaDand tropomyosin together prevent actin filaments from bundling. The presence of Ca^{2+}-CaM is required in the ternary structure of actin, tropomyosin and CaD to regulate CaD activity so that tropomyosin and CaD are in the appropriate position to allow the binding of fascin to actin filaments (Ishikawa et al., 1998), leading to assembly of stress fibers. Once stress fibers are formed, associated CaD can stabilize the structures and prevent it from disassembly, possibly by inhibiting the activities of actin-severing proteins such as gelosin (Ishikawa et al., 1989b) and cofilin (Yamashiro et al., 2001). It is likely that the requirement of Ca^{2+}-CaM for actin bundling is transient, in which case Ca^{2+}-CaM would be released after assembly of stress fibers, allowing it to regulate CaD activity in a temporally and spatially specific way. Taken together, CaD plays dual roles in actin dynamics: first, in the regulation of bundling protein activity and, second, in the stabilization of stress fiber structures in the presence of Ca^{2+}-CaM.

Mutant CaD39-AB functionally competes with the endogenous CHO CaD in the overexpressing cells

When overexpressed in CHO cells, CaD39-AB might integrate randomly into actin filaments and prohibit bundling in the presence of tropomyosin, whereas actin filaments associated with endogenous CaD can bundle together to form few stress fibers through Ca^{2+}-CaM regulation. Because the expression

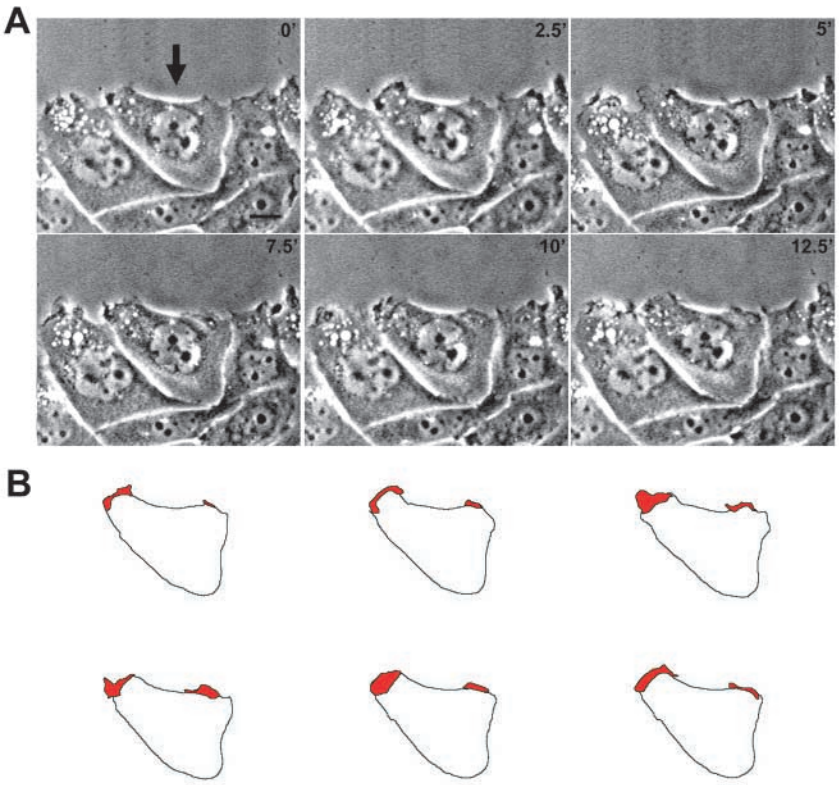

Fig. 13. Phase-contrast images and outlines of migrating mutant m5-8 cells during wound healing. Derived from original video taping, the phase-contrast images (A) of migrating cells starts 2.5 hours after wounding and continues for 12.5 minutes at intervals of 2.5 minutes. (B) The outlines of a representative cell (A, arrow) in which membrane extension zones are filled with red. Small, discrete membrane extensions were observed in CaD39-AB-expressing cells. Scale bar, 10 μm.

level of the endogenous CaD is less than that of CaD39-AB (less than 1/80th of the level), force-expressed CaD39-AB will be functionally competing with the endogenous CaD in the overexpressing cells, which locks actin filaments in an inhibitory conformation for actin bundling and leads to the disintegration of stress fibers in overexpressing cells.

It is noteworthy that the disruption of stress fiber assembly in overexpressing cells accompanies disruption of focal-adhesion structures. The association of focal adhesions with CaD39-AB-containing microfilaments that are not bundling might result in poor colocalization between vinculin and stress fibers. Moreover, it has been shown that formation of focal adhesions is dependent on the development of tension generated in the actomyosin system (Kaverina et al., 2002). Inhibition of actomyosin ATPase by CaD39-AB, along with the disruption of actin integrity in overexpressing cells, might result in insufficient tension within the actomyosin system for the formation/stabilization of focal adhesion structures. The diffused staining of CaD39-AB and the disorganized structures of stress fibers and focal adhesions in the overexpressing clones resemble the phenotypes that Helfman et al. (Helfman et al., 1999) observed in their transient expression of wild-type CaD. They showed that the expression of full-length CaD in fibroblasts inhibits the assembly of stress fibers, disrupts focal adhesions and causes a defect in cell contractility, all of which can be reversed by elevated cytoplasmic Ca^{2+} concentrations.

Regulation of CaD by Ca^{2+}-CaM is crucial in maintaining cytoskeleton integrity and proper cell contractility for cell morphology, growth and motility

Coincident with disruption of stress fibers and focal adhesions, expression of CaD39-AB delays cell-cycle progression and alters cell morphology. The CaD39-AB-overexpressing cells grow much more slowly and exhibit a larger and less polarized cell shape than the parent CHO cells or CaD39-overexpressing cells. The defects in cell shape and cell cycle probably result from the disruption of stress fibers and focal adhesions by CaD39-AB mutant protein. It has been shown that disruption of stress fibers by cytochalasin D inhibits the synthesis of DNA, RNA and proteins, as well as S-phase entry (Iwig et al., 1995). Furthermore, cytochalasin D also blocks growth-factor-induced expression of cyclin D1 and phosphorylation of pRb (Bohmer et al., 1996). It is thus believed that an intact cytoskeleton system is important in the cyclin/cyclin-dependent-kinase pathway, possibly by modulating the proper localization of G1-phase regulators (Lohez et al., 2003). Disruption of stress fibers in overexpressing cells might result in a delay in the G1/M-phase transition, thus slowing down cell-cycle progression. Meanwhile, disintegrated stress fibers and focal adhesions might impair the generation of proper tension in the cortical cytoskeleton required for maintaining the polygonal shape of CHO cells. Because Ca^{2+}-CaM cannot reverse the inhibitory effect of CaD39-AB on myosin ATPase activity, cell contractility would be greatly impaired by the expression of CaD39-AB mutant, which in turn leads to a rounder, larger cell.

Disorganized microfilaments and weakened contractility also contribute to the motility defects of CaD39-AB-expressing cells in the wound-healing assay. It has been shown that the actin network is highly organized during migration. Within the cell body, actin is highly organized into fibers either perpendicular or parallel to the direction of cell migration. Transverse fibers perpendicular to the direction of migration produce contractions that narrow the anterior portion of a migrating cell and induce detachment from neighboring cells (Hahn et al., 1992), whereas stress fibers aligned with direction of translocation provide contraction along the axis of movement that contributes to forward migration (Wang, 1984). Lack of integrated stress fibers, together with a deficiency in myosin ATPase activity, might impair the generation of coordinated contractility across the cell body and therefore slow down cell movement. Moreover, it has been shown that changes in actin organization and cytoskeleton-based contraction forces are crucial to the orientation of lamella extension and the direction of cell migration (Parker et al., 2002).

During wound healing, membrane extension in CaD39-AB-expressing cells is not as active as in control cells. Instead of producing a broad lamellipodium over the front edge, a CaD39-AB-expressing cell extends small multiple protrusions. Immunofluorescence microscopy has showed concentrated CaD39-AB staining at the leading edge during wound healing (data not shown). In addition, Ca^{2+}-CaM is known to concentrate in the lamellipodia during the period that we monitored wound healing (Hahn et al., 1992). Therefore, defects in membrane extension might be directly caused by the presence of CaD39-AB within the lamellipodia, which affects actin bundling and/or actin polymerization. Portions of lamellipodia contain bundles of actin filaments called microspikes (Ballestrem et al., 1998), and actin-bundling proteins such as fascin are believed to play an important role in their assembly (Small et al., 2002). It is possible that CaD39-AB at the leading edge inhibits bundling activity, suppresses the formation of microspikes and thus destabilizes the structure of membrane protrusion (Fisher et al., 1988). Alternatively, but not exclusively, in vitro studies have demonstrated that CaD inhibits Arp2/3-induced actin polymerization and that this inhibition can be reversed by Ca^{2+}-CaM (Yamakita et al., 2003). Loss of regulation by Ca^{2+}-CaM might allow CaD39-AB to inhibit Arp2/3 activity at the leading edge, which might in turn reduce membrane protrusion (Pollard et al., 2000).

Taken together, our results have identified Ca^{2+}-CaM as a key regulator of CaD activity. Regulation of CaD by Ca^{2+}-CaM plays an important role in the assembly of stress fibers, in the generation of cell contractility and probably also in Arp2/3-induced polymerization of actin. Furthermore, motility defects shown in CaD39-AB-expressing cells resemble those observed in CaM-deficient cells (Walker et al., 1998), suggesting that CaD is involved in Ca^{2+}-CaM control of cell locomotion.

We thank D. Wessels for constructive discussion and J.-Y. Choi, W. Pierce and J. Sholley for their great technical assistance. This work is supported by grant HD18577 from the US National Institutes of Health and a grant from the W. M. Keck Foundation.

References

Ballestrem, C., Wehrle-Haller, B. and Imhof, B. (1998). Actin dynamics in living mammalian cells. *J. Cell Sci.* **111**, 1649-1658.

Bohmer, R. M., Scharf, E. and Assoian, R. K. (1996). Cytoskeletal integrity is required throughout the mitogen stimulation phase of the cell cycle and mediates the anchorage-dependent expression of cyclin D1. *Mol. Biol. Cell* **7**, 101-111.

Cheng, S., Geddis, M. S. and Rehder, V. (2002). Local calcium changes regulate the length of growth cone filopodia. *J. Neurobiol.* **50**, 263-275.

Chin, D. and Means, A. R. (2000). Calmodulin: a prototypical calcium sensor. *Trends Cell Biol.* **10**, 322-328.

Fisher, G. W., Conrad, P. A., Debiasio, R. L. and Taylor, D. L. (1988). Centripetal transport of cytoplasm, actin, and the cell-surface in lamellipodia of fibroblasts. *Cell Motil. Cytoskeleton* **11**, 235-247.

Fraser, I. D., Copeland, O., Bing, W. and Marston, S. B. (1997). The inhibitory complex of smooth muscle caldesmon with actin and tropomyosin involves three interacting segments of the C-terminal domain 4. *Biochemistry* **36**, 5483-5492.

Gough, A. H. and Taylor, D. L. (1993). Fluorescence anisotropy imaging microscopy maps calmodulin-binding during cellular contraction and locomotion. *J. Cell Biol.* **121**, 1095-1107.

Graether, S. P., Heinonen, T. Y., Raharjo, W. H., Jin, J. P. and Mak, A. S. (1997). Tryptophan residues in caldesmon are major determinants for calmodulin binding. *Biochemistry* **36**, 364-369.

Hahn, K., Debiasio, R. and Taylor, D. L. (1992). Patterns of elevated free calcium and calmodulin activation in living cells. *Nature* **359**, 736-738.

Hayashi, K., Yano, H., Hashida, T., Takeuchi, T., Takeda, O., Asada, K., Takashashi, E., Kato, I. and Sobue, K. (1992). Genomic structure of the human caldesmon gene. *Proc. Nat. Acad. Sci. USA* **89**, 12122-12126.

Helfman, D. M., Levy, E. T., Berthier, C., Shtutman, M., Riveline, D., Grosheva, I., Lachish-Zalait, A., Elbaum, M. and Bershadsky, A. D. (1999). Caldesmon inhibits nonmuscle cell contractility and interferes with the formation of focal adhesions. *Mol. Biol. Cell* **10**, 3097-3112.

Horton, R. M., Hunt, H. D., Ho, S. N., Pullen, J. K. and Pease, L. R. (1989). Engineering hybrid genes without the use of restriction enzymes – gene-splicing by overlap extension. *Gene* **77**, 61-68.

Huber, P. A., Gao, Y., Fraser, I. D., Copeland, O., El-Mezgueldi, M., Slatter, D. A., Keane, N. E., Marston, S. B. and Levine, B. A. (1998a). Structure-activity studies of the regulatory interaction of the 10 kiloDalton C-terminal fragment of caldesmon with actin and the effect of mutation of caldesmon residues 691-696. *Biochemistry* **37**, 2314-2326.

Huber, P. A., Levine, B. A., Copeland, O., Marston, S. B. and El-Mezgueldi, M. (1998b). Characterisation of the effects of mutation of the caldesmon sequence ^{691}Glu-Trp-Leu-Thr-Lys-Thr^{696} to Pro-Gly-His-Tyr-Asn-Asn on caldesmon-calmodulin interaction. *FEBS Lett.* **423**, 93-97.

Humphrey, M. B., Herrera-Sosa, H., Gonzalez, G., Lee, R. and Bryan, J. (1992). Cloning of cDNAs encoding human caldesmon. *Gene* **112**, 197-204.

Ishikawa, R., Yamashiro, S. and Matsumura, F. (1989a). Annealing of gelsolin-severed actin fragments by tropomyosin in the presence of Ca^{2+}. *J. Biol. Chem.* **264**, 16764-16770.

Ishikawa, R., Yamashiro, S. and Matsumura, F. (1989b). Differential modulation of actin-severing activity of gelsolin by multiple isoforms of cultured rat cell tropomyosin: potentiation of protective ability of tropomyosins by 83-kDa nonmuscle caldesmon. *J. Biol. Chem.* **264**, 7490-7497.

Ishikawa, R., Yamashiro, S., Kohama, K. and Matsumura, F. (1998). Regulation of actin binding and actin bundling activities of fascin by caldesmon coupled with tropomyosin. *J. Biol. Chem.* **273**, 26991-26997.

Iwig, M., Czeslick, E., Muller, A., Gruner, M., Spindler, M. and Glaesser, D. (1995). Growth-regulation by cell-shape alteration and organization of the cytoskeleton. *Eur. J. Cell Biol.* **67**, 145-157.

Kaverina, I., Krylyshkina, O. and Small, J. V. (2002). Regulation of substrate adhesion dynamics during cell motility. *Int. J. Biochem. Cell Biol.* **34**, 746-761.

Li, Y., Wessels, D., Wang, T., Lin, J. L. C., Soll, D. R. and Lin, J. J. C. (2003). Regulation of caldesmon activity by Cdc2 kinase plays an important role in maintaining membrane cortex integrity during cell division. *Cell. Mol. Life Sci.* **60**, 198-211.

Lin, J. J. C., Yamashiro-Matsumura, S. and Matsumura, F. (1984). Microfilaments in normal and transformed cells: changes in the multiple forms of tropomyosin. *Cancer Cells* **1**, 57-65.

Lin, J. J. C., Davis-Nanthakumar, E. J., Jin, J. P., Lourim, D., Novy, R. E. and Lin, J. L. C. (1991). Epitope mapping of monoclonal antibodies against caldesmon and their effects on the binding of caldesmon to Ca^{2+}/calmodulin and to actin or actin-tropomyosin filaments. *Cell Motil. Cytoskeleton* **20**, 95-108.

Lohez, O. D., Reynaud, C., Borel, F., Andreassen, P. R. and Margolis, R. L. (2003). Arrest of mammalian fibroblasts in G1 in response to actin inhibition is dependent on retinoblastoma pocket proteins but not on p53. *J. Cell Biol.* **161**, 67-77.

Marston, S. B. and Redwood, C. S. (1991). The molecular anatomy of caldesmon. *Biochem. J.* **279**, 1-16.

Marston, S. B., Fraser, I. D. C., Huber, P. A. J., Pritchard, K., Gusev, N. B. and Torok, K. (1994). Location of two contact sites between human caldesmon and Ca^{2+}/calmodulin. *J. Biol. Chem.* **269**, 8134-8139.

Marston, S., Burton, D., Copeland, O., Fraser, I., Gao, Y., Hodgkinson, J., Huber, P., Levine, B., El-Mezgueldi, M. and Notarianni, G. (1998). Structural interactions between actin, tropomyosin, caldesmon and calcium binding protein and the regulation of smooth muscle thin filaments. *Acta Physiol. Scand.* **164**, 401-414.

Matsumura, F., Yamashiro-Matsumura, S. and Lin, J. J. C. (1983). Isolation and characterization of tropomyosin-containing microfilaments from cultured cells. *J. Biol. Chem.* **258**, 6636-6644.

Mezgueldi, M., Derancourt, J., Calas, B., Kassab, R. and Fattoum, A. (1994). Precise identification of the regulatory F-actin-binding and calmodulin-binding sequences in the 10-kDa carboxyl-terminal domain of caldesmon. *J. Biol. Chem.* **269**, 12824-12832.

Notarianni, G., Gusev, N., Lafitte, D., Hill, T. J., Cooper, H. S., Derrick, P. J. and Marston, S. B. (2000). A novel Ca^{2+} binding protein associated with caldesmon in Ca^{2+}-regulated smooth muscle thin filaments: evidence

for a structurally altered form of calmodulin. *J. Muscle Res. Cell Motil.* **21**, 537-549.

Novy, R. E., Sellers, J. R., Liu, L. F. and Lin, J. J. C. (1993). In vitro functional characterization of bacterially expressed human fibroblast tropomyosin isoforms and their chimeric mutants. *Cell Motil. Cytoskeleton* **26**, 248-261.

Parker, K. K., Brock, A. L., Brangwynne, C., Mannix, R. J., Wang, N., Ostuni, E., Geisse, N. A., Adams, J. C., Whitesides, G. M. and Ingber, D. E. (2002). Directional control of lamellipodia extension by constraining cell shape and orienting cell tractional forces. *FASEB J.* **16**, 1195-1204.

Pollard, T. D., Blanchoin, L. and Mullins, R. D. (2000). Molecular mechanisms controlling actin filament dynamics in nonmuscle cells. *Annu. Rev. Biophys. Biomol. Struct.* **29**, 545-576.

Pritchard, K., Smith, C. W. J., Moody, C. J. and Marston, S. B. (1987). The caldesmon/calmodulin system in the Ca^{2+}-regulation of smooth-muscle thin-filaments. *J. Muscle Res. Cell Motil.* **8**, 78.

Ranta-Knuuttila, T., Kiviluoto, T., Mustonen, H., Puolakkainen, P., Watanabe, S., Sato, N. and Kivilaakso, E. (2002). Migration of primary cultured rabbit gastric epithelial cells requires intact protein kinase C and Ca^{2+}/calmodulin activity. *Dig. Dis. Sci.* **47**, 1008-1014.

Shirinsky, V. P., Biryukov, K. G., Hettasch, J. M. and Sellers, J. (1992). Inhibition of the relative movement of actin and myosin by caldesmon and calponin. *J. Biol. Chem.* **267**, 15886-15892.

Small, J. V., Stradal, T., Vignal, E. and Rottner, K. (2002). The lamellipodium: where motility begins. *Trends Cell Biol.* **12**, 112-120.

Smith, C. W. J., Pritchard, K. and Marston, S. B. (1987). The mechanism of Ca^{2+} regulation of vascular smooth-muscle thin-filaments by caldesmon and calmodulin. *J. Biol. Chem.* **262**, 116-122.

Sobue, K., Kanda, K., Adachi, J. and Kakiuchi, S. (1983). Calmodulin-binding proteins that interact with actin-filaments in a Ca^{2+}-dependent flip-flop manner – survey in brain and secretory-tissues. *Proc. Nat. Acad. Sci. USA* **80**, 6868-6871.

Soll, D. R. (1995). The use of computers in understanding how animal cells crawl. *Int. Rev. Cytol.* **8**, 439-454.

Soll, D. R. and Voss, E. (1998). Two and three-dimensional computer systems for analyzing how cells crawl. In *Motion Analysis of Living Cells* (eds D. R. Soll and D. Wessels), pp. 25-52. New York, NY: Wiley-Liss.

Walker, J. W., Gilbert, S. H., Drummond, R. M., Yamada, M., Sreekumar, R., Carraway, R. E., Ikebe, M. and Fay, F. S. (1998). Signaling pathways underlying eosinophil cell motility revealed by using caged peptides. *Proc. Nat. Acad. Sci. USA* **95**, 1568-1573.

Wang, Y. L. (1984). Reorganization of actin filament bundles in living fibroblasts. *J. Cell Biol.* **99**, 1478-1485.

Wang, Z. and Chacko, S. (1996). Mutagenesis analysis of functionally important domains within the C-terminal end of smooth muscle caldesmon. *J. Biol. Chem.* **271**, 25707-25714.

Wang, Z., Yang, Z. Q. and Chacko, S. (1997). Functional and structural relationship between the calmodulin-binding, actin-binding, and actomyosin-ATPase inhibitory domains on the C-terminus of smooth muscle caldesmon. *J. Biol. Chem.* **272**, 16896-16908.

Warren, K. S., Lin, J. L., Wamboldt, D. D. and Lin, J. J. (1994). Overexpression of human fibroblast caldesmon fragment containing actin-, Ca^{2+}/calmodulin-, and tropomyosin-binding domains stabilizes endogenous tropomyosin and microfilaments. *J. Cell Biol.* **125**, 359-368.

Warren, K. S., Shutt, D. C., McDermott, J. P., Lin, J. L., Soll, D. R. and Lin, J. J. (1996). Overexpression of microfilament-stabilizing human caldesmon fragment, CaD39, affects cell attachment, spreading, and cytokinesis. *Cell Motil. Cytoskeleton* **34**, 215-229.

Yamakita, Y., Oosawa, F., Yamashiro, S. and Matsumura, F. (2003). Caldesmon inhibits Arp2/3-mediated actin nucleation. *J. Biol. Chem.* **278**, 17937-17944.

Yamashiro, S., Chen, H., Yamakita, Y. and Matsumura, F. (2001). Mutant caldesmon lacking Cdc2 phosphorylation sites delays M-phase entry and inhibits cytokinesis. *Mol. Biol. Cell* **12**, 239-250.

Yamashiro-Matsumura, S. and Matsumura, F. (1988). Characterization of 83-kiloDalton nonmuscle caldesmon from cultured rat cells: stimulation of actin binding of nonmuscle tropomyosin and periodic localization along microfilaments like tropomyosin. *J. Cell Biol.* **106**, 1973-1983.

Zhan, Q., Wong, S. S. and Wang, C. L. A. (1991). A calmodulin-binding peptide of caldesmon. *J. Biol. Chem.* **266**, 21810-21814.